ChemComm

COMMUNICATION

View Article Online
View Journal

Cite this: DOI: 10.1039/d0cc07858a

Received 2nd December 2020,
Accepted 21st January 2021

DOI: 10.1039/d0cc07858a

rsc.li/chemcomm

Radical-triggered cross-linking for molecular layer deposition of SiAlCOH hybrid thin films†

Kristina Ashurbekova, [a] Karina Ashurbekova,*[b] Iva Saric, [c] Evgeny Modin,[b] Mladen Petravic,[c] Ilmutdin Abdulagatov,[a] Aziz Abdulagatov[a] and Mato Knez *[bcd]

Here, we report on a simultaneous growth and radical-initiated cross-linking of a hybrid thin film in a layer-by-layer manner *via* molecular layer deposition (MLD). The cross-linked film exhibited a self-limiting MLD growth behavior and improved properties like 12% higher film density and enhanced stability compared to the non-cross-linked film.

Stable ultrathin organic and hybrid thin films are desirable materials due to their ubiquitous applications. With vapor phase coating processes, the films often grow as arrays of individual molecular chains with limited thermal or mechanical stability. For improving the stability, cross-linking of the chains is the optimal choice.

The outstanding chemical and physical properties of siloxane-based materials, such as high failure to strain, low elastic moduli,[1] or hydrophobicity and chemical inertness[2,3] have made these materials ubiquitous in science and technology. They find application in microelectronics as dielectric layers,[4,5] bioinert coatings,[6–8] or thin-film encapsulators.[9] Silicon-based polymers can also be converted into a special class of high-temperature materials known as polymer-derived ceramics (PDCs).[10,11] Aluminum doped SiOC PDC's, obtained using solution chemistry, showed increased creep and corrosion resistance of the final material.[12] For all of the above-mentioned applications, it is beneficial to cross-link the deposited films. The advantages of cross-linking include enhancement of the mechanical strength,[13] thermal stability,[14] and density of the film. Previous studies of siloxane-type films, grown by chemical vapor deposition (CVD), demonstrated the strong dependence of the film stability on the degree of cross-linking.[15] In CVD, the vinyl-functionalized silanes/siloxanes are commonly cross-linked with di-*tert*-butyl peroxide, cracked into radicals by a hot filament, as a free-radical-generating initiator.[6] In the case of molecular layer deposition (MLD), cross-linking still remains a challenge. Bent's group demonstrated that a series of multiamines can be used to grow polyurea films by MLD urea-coupling reactions.[16] They showed that the cross-linking indeed improved the film properties. Cross-linking of vinyl groups simultaneous to growing MLD films is a scientific and technical challenge and was not demonstrated so far.

The MLD process is a vapor phase technique developed for organic and hybrid organic–inorganic thin film growth. MLD enables conformal growth of ultrathin and ultrasmooth films with molecular level thickness and composition control.[17–20] Siloxane-type films can be grown by MLD. Recently, we have demonstrated the growth of such films following ring-opening polymerization (ROP) reactions of trivinyl-trimethylcyclotrisiloxane (V_3D_3) and azasilane.[21] Also, the MLD of a siloxane–alumina hybrid film, using a two-step process including TMA and 2,4,6,8-tetramethyl-2,4,6,8-tetravinylcyclotetrasiloxane (V_4D_4) as precursors, was presented.[22]

In the present work, di-*tert*-butyl peroxide (TBPO) has been used to perform cross-linking of the V_4D_4 through their vinyl side chains simultaneously with the growth of the (V_4D_4)-TMA alumosiloxane film by MLD.

The proposed scheme of the three-step MLD process is shown in Fig. 1. Cross-linking was achieved by introducing a third precursor, TBPO, into the process (Fig. 1). The TBPO was dosed after V_4D_4, with the pulsing sequence being V_4D_4/TBPO/TMA. Reaction (A) represents an anchoring of V_4D_4 to the aluminum-methylated surface upon ring-opening of V_4D_4 and binding of the chain to the aluminum through oxygen. In step (B), thermal decomposition of TBPO occurs,[23] which generates radicals, attacking the vinyl groups on silicon, thereby forming methylene groups and consequently –Si–CHR–CHR–Si– bridges, where R is $CH_2OC(CH_3)_3$ as shown in the inset in Fig. 1. The reaction (C) of TMA with the cross-linked V_4D_4 units occurs in a similar way as in the two-step V_4D_4/TMA MLD

[a] *Dagestan State University, Makhachkala 36700, Russian Federation. E-mail: krashurbekova@inbox.ru*
[b] *CIC nanoGUNE, Donostia-San Sebastián E-20018, Spain. E-mail: m.knez@nanogune.eu*
[c] *University of Rijeka, Department of Physics and Centre for Micro- and Nanosciences and Technologies, Rijeka 51000, Croatia*
[d] *IKERBASQUE, Basque Foundation for Science, Bilbao E-48013, Spain*

† Electronic supplementary information (ESI) available. See DOI: 10.1039/d0cc07858a

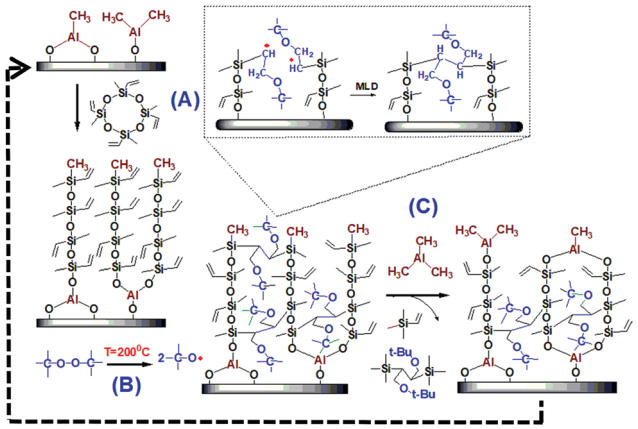

Fig. 1 Schematic of the alumosiloxane MLD growth from V_4D_4 and TMA, including cross-linking of the chains with di-*tert*-butyl peroxide (TBPO).

process.[22] TMA may also attack the C–O–C bonds of the newly formed $-CH_2OC(CH_3)_3$ groups from decomposed TBPO.

Fig. 2(a) shows the observed QCM mass change *vs.* time during 20 cycles of V_4D_4/TBPO/TMA MLD at 200 °C. For the deposition, the 6/22/2/22/2/22 second timing sequence has been used for pulsing and purging of V_4D_4, TBPO and TMA, respectively. A linear and reproducible mass increase over the MLD cycle numbers was observed. The inset in Fig. 2(a) shows an expanded view of the QCM signal during the three-step MLD process at 200 °C. From the figure, the total mass gain per cycle (MGPC) was 18 ng cm^{-2}. The QCM signal shows that each precursor dose results in a mass increase. The V_4D_4, TBPO and TMA doses lead to a mass gain of 12, 4 and 2 ng cm^{-2}, respectively. For QCM studies of the self-limiting surface chemistry of the individual reactions, see Fig. 1S in the ESI.† Exceeding the dosing times beyond 6, 2 and 2 seconds did not result in a higher mass gain. The mass gain after the TBPO dose is consistent with the proposed reaction mechanism and suggests a radical formation and chain cross-linking. A big spike observed during the TBPO dose is most likely related to a temperature transient[24] and/or TBPO diffusion into the bulk of the MLD film.[25] At 150 °C, we did not observe a mass gain with the TBPO dose, which is likely due to its thermal stability (*viz.* lack of decomposition) at those temperatures (Fig. 2S, ESI†).

Fig. 2(b) shows a comparison of the attenuated total reflectance Fourier transform infrared (ATR-FTIR) spectra of the 400 Å thick film, deposited at 200 °C using a two-step V_4D_4/TMA MLD, and of the cross-linked 450 Å thick film, deposited at 200 °C using a three-step V_4D_4/TBPO/TMA MLD process. A background spectrum of pure ZrO_2 nanoparticles was recorded initially and was subtracted from the sample spectra. An intensity decrease of the vinyl signals, such as $=CH_2$ deformation at 1409 cm^{-1}, $=CH_2$ stretching at 3055 cm^{-1}, and $=CH$ stretching at 2930 cm^{-1}, can be noticed. The peak at 1460 cm^{-1} in the cross-linked film is associated with asymmetric $-CH_2$ bending from the newly formed methylene groups in the –Si–CHR–CHR–Si– bridges, where R is $CH_2OC(CH_3)_3$.[26–28] The $=CH_2$ band at 1409 cm^{-1} is still present in the spectrum of the cross-linked film, indicating that not all vinyl groups reacted.

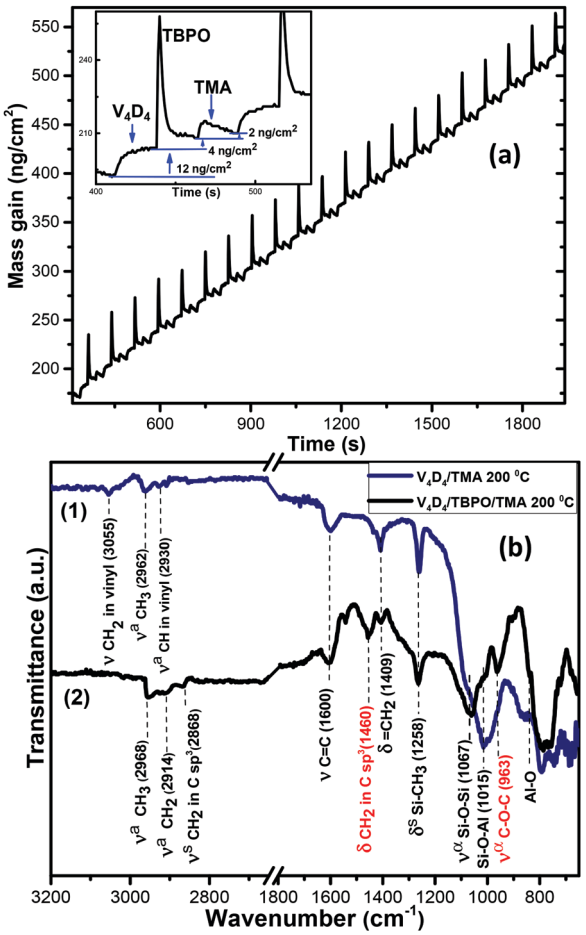

Fig. 2 (a) QCM mass gain *versus* time for an MLD process using V_4D_4, TBPO, and TMA: growth over 20 reaction cycles in a steady-state regime at 200 °C. The inset shows an expanded view of the mass gain during two reaction cycles. (b) ATR-FTIR spectra of (1) 400 Å thick alumosiloxane film, deposited on pressed ZrO_2 particles at 200 °C using a two-step V_4D_4/TMA MLD; (2) cross-linked 450 Å thick alumosiloxane film, deposited on ZrO_2 particles at 200 °C using a three-step V_4D_4/TBPO/TMA process.

Also, this band is attributed to newly generated methylene groups within the film.[6] Another peak at 963 cm^{-1} in the cross-linked MLD film is attributed to asymmetric C–O–C stretching vibrations,[29] even though the C–O–C stretch is typically observed at higher wavenumbers around 1200–1000 cm^{-1}. The 1000–1150 cm^{-1} region of spectrum (2) is shifted to higher wavenumbers relative to spectrum (1) in Fig. 2. The Si–O–Si peak at 1067 cm^{-1}, that appeared as shoulder in spectrum (1), appears as a peak in spectrum (2). A small shoulder at 1105 cm^{-1} that is seen on the Si–O–Si peak could be the overlapped C–O–C stretch. The appearance of a C–O–C peak is additional evidence of TBPO species incorporation in agreement with the proposed reaction scheme. Other functional groups do not undergo any changes upon the added TBPO step.

A constant growth of 1.8 Å/cycle was obtained for the cross-linked V_4D_4/TBPO/TMA film deposited on Si(100) at 200 °C. The resulting film density of 2.5 g cm^{-3}, as determined from the X-ray reflectivity (XRR) measurements, is 12% higher than that of the V_4D_4/TMA film (2.2 g cm^{-3}) deposited at the same

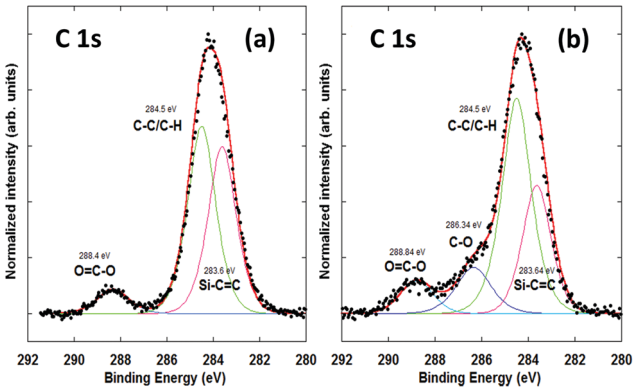

Fig. 3 XPS spectra around the C 1s core-level of (a) a 210 Å thick film deposited at 200 °C using a two-step V_4D_4/TMA process and (b) a cross-linked 240 Å thick film deposited using the three-step V_4D_4/TBPO/TMA process.

temperature, indicating a denser packing of the V_4D_4/TBPO/TMA film due to the cross-linking (Fig. 3S, ESI†). A root mean square (RMS) roughness of 5.4 Å was obtained for the 250 Å thick cross-linked alumosiloxane film. (Fig. 3S, ESI†)

Fig. 3 shows a comparison of high-resolution C 1s X-ray photoelectron spectroscopy (XPS) spectra of silicon wafers coated with (a) a 210 Å thick V_4D_4/TMA film and (b) a cross-linked 240 Å thick V_4D_4/TBPO/TMA film grown at 200 °C. The spectrum in Fig. 3(a) was deconvoluted into three components, assigned to the Si–C═C, C–C/C–H, and O═C–O (surface contamination) bonding arrangement of carbon at BEs of 283.6, 284.5 and 288.8 eV, respectively.[30] A new peak in the spectrum from the cross-linked film in Fig. 3(b) at 286.3 eV is attributed to C–O bonds. This new peak indicates the incorporation of TBPO species into the film and thus cross-linking. The Al 2p and Si 2p spectra of the cross-linked film were identical to those of the V_4D_4/TMA film.[22]

Finally, transmission electron microscopy (TEM) was used to visualize the conformality of the alumosiloxane thin film coatings. Fig. 4 shows a TEM image of ZrO_2 nanoparticles (NPs) coated with a 55 Å thick cross-linked MLD film, obtained from the three-step V_4D_4/TBPO/TMA process at 200 °C, using the timing sequence of 6/22/2/22/2/22 to fulfill a self-saturated condition. ZrO_2 NPs were used because of their high surface area and good contrast in TEM. The micrograph in Fig. 4 shows conformally coated NPs, confirming a successful MLD process. The growth of 1.75 Å cycle^{-1}, as obtained from the TEM image, is in good agreement with the value obtained from XRR, namely 1.8 Å cycle^{-1}. The TEM images further confirm the amorphous nature of the deposited film.

The stability of the films was assessed through thermal treatment of the samples and the evaluation of the changes in the film thickness, measured using XRR. Fig. 5 shows alumosiloxane film thickness changes after annealing in air at various temperatures for 1 hour. Annealing of the 150 °C-deposited V_4D_4/TMA film at 1100 °C resulted in a 47% loss in thickness, while the same thermal treatment of the 200 °C-deposited V_4D_4/TMA film exhibited a 29% thickness loss. The highest stability was observed from the cross-linked V_4D_4/TBPO/TMA film,

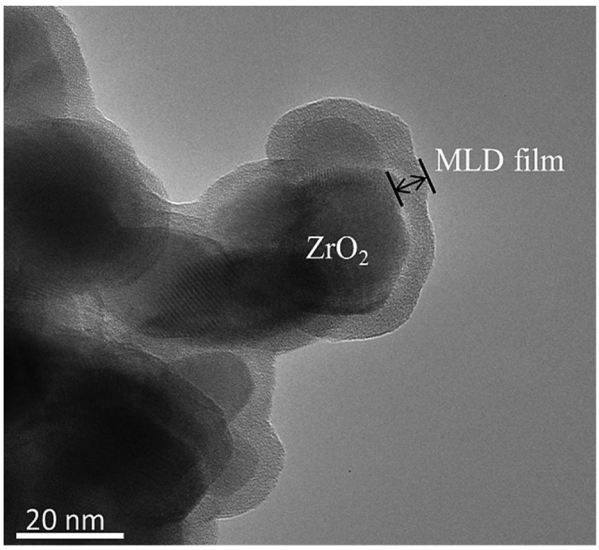

Fig. 4 TEM image of ZrO_2 NPs coated with 55 Å thick MLD film, deposited using the three-step V_4D_4/TBPO/TMA process at 200 °C with the timing sequence of 6/22/2/22/2/22.

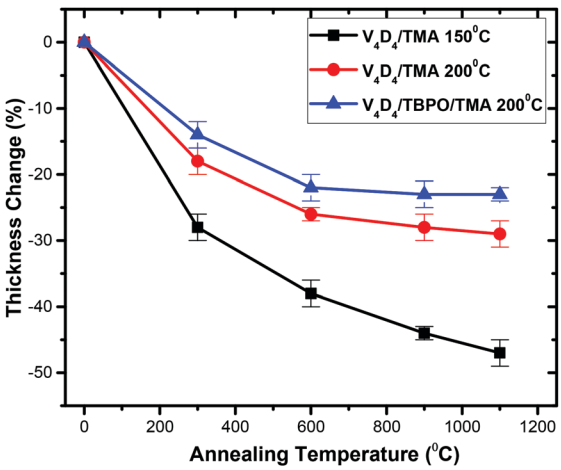

Fig. 5 Alumosiloxane film thickness changes after annealing in air at various temperatures for 1 hour. Thickness changes were compared for V_4D_4/TMA films deposited at 150 °C (black) and 200 °C (red) and cross-linked V_4D_4/TBPO/TMA deposited at 200 °C (blue).

deposited at 200 °C, with only 23% thickness loss after annealing at 1100 °C for 1 hour.

In summary, in this study, cross-linking of MLD-grown alumosiloxane films was achieved by introducing a third precursor, di-*tert*-butyl peroxide (TBPO), into the MLD process at 200 °C processing temperature. A constant growth per cycle and a self-limiting nature of the performed MLD reactions were demonstrated by *in situ* QCM studies. The presence of characteristic IR peaks of methylene groups in –Si–CHR–CHR–Si– bridges, where R is $CH_2OC(CH_3)_3$, as well as an increase in the intensity of the C–O component in the XPS C 1s spectrum, confirm an effective cross-linking of the vinyl groups by TBPO and the formation of 3D networks in the film. TEM showed

growth of a highly conformal film on zirconia nanoparticles. The developed process shows the first MLD-based radical-induced cross-linking approach and is transferrable to other MLD systems that contain chemical groups with unsaturated bonds. The obtained cross-linked MLD film exhibited a thickness loss of 23% after annealing in air at 1100 °C for one hour and 12% higher film density compared to the same film without a cross-linking step. The cross-linking is expected to also enhance the mechanical stability of the deposited films, which is the subject of our ongoing research.

The manuscript was written through the contributions of all authors. All authors have approved the final version of the manuscript.

M. K. is grateful for funding from the Spanish Ministry of Science and Innovation (MICINN) [Grant Agreement No. PID2019-111065RB-I00], including FEDER funds, and the Maria de Maeztu Units of Excellence Programme [grant number MDM-2016-0618]. Ka. A. acknowledges funding through EU Horizon 2020 research and innovation programme under the Marie Sklodowska-Curie grant agreement No. 765378. I. A. and Kr. A. acknowledge funding through the Russian Federation government under the grant number FZNZ-2020-0002. I. S. and M. P. acknowledge support from the University of Rijeka under project number 18-144.

Conflicts of interest

There are no conflicts to declare.

References

1 N. Takano, T. Fukuda and K. Ono, *Polym. J.*, 2001, **33**, 469–474.
2 H. Zhou and S. F. Bent, *J. Phys. Chem. C*, 2013, **117**, 19967–19973.
3 R. G. Closser, D. S. Bergsman and S. F. Bent, *ACS Appl. Mater. Interfaces*, 2018, **10**, 24266–24274.
4 H. Moon, H. Seong, W. C. Shin, W.-T. Park, M. Kim, S. Lee, J. H. Bong, Y.-Y. Noh, B. J. Cho, S. Yoo and S. G. Im, *Nat. Mater.*, 2015, **14**, 628.
5 K. Pak, H. Seong, J. Choi, W. Hwang and S. Im, *Adv. Funct. Mater.*, 2016, 26.
6 W. S. O'Shaughnessy, M. Gao and K. K. Gleason, *Langmuir*, 2006, **22**, 7021–7026.
7 W. S. O'Shaughnessy, S. K. Murthy, D. J. Edell and K. K. Gleason, *Biomacromolecules*, 2007, **8**, 2564–2570.
8 A. Achyuta, V. S. Polikov, A. White, H. P. Lewis and S. K. Murthy, *Macromol. Biosci.*, 2010, **10**, 872–880.
9 B. J. Kim, H. Seong, H. Shim, Y. I. Lee and S. Im, *Adv. Eng. Mater.*, 2017, 19.
10 P. Colombo, G. Mera, R. Riedel and G. D. Sorarù, *J. Am. Ceram. Soc.*, 2010, **93**, 1805–1837.
11 G. Barroso, Q. Li, R. K. Bordia and G. Motz, *J. Mater. Chem. A*, 2019, **7**, 1936–1963.
12 Z. C. Eckel, C. Zhou, J. H. Martin, A. J. Jacobsen, W. B. Carter and T. A. Schaedler, *Science*, 2016, **351**, 58–62.
13 L. Richert, A. J. Engler, D. E. Discher and C. Picart, *Biomacromolecules*, 2004, **5**, 1908–1916.
14 K. Chan and K. K. Gleason, *Langmuir*, 2005, **21**, 8930–8939.
15 D. D. Burkey and K. K. Gleason, *J. Electrochem. Soc.*, 2004, **151**, F105.
16 H. Zhou, M. F. Toney and S. F. Bent, *Macromolecules*, 2013, **46**, 5638–5643.
17 S. M. George, B. Yoon and A. A. Dameron, *Acc. Chem. Res.*, 2009, **42**, 498–508.
18 K. Ashurbekova, Kr. Ashurbekova, G. Botta, O. Yurkevich and M. Knez, *Nanotechnology*, 2020, **31**, 342001.
19 G. N. Parsons, S. M. George and M. Knez, *MRS Bull.*, 2011, **36**, 865–871.
20 X. Meng, *J. Mater. Chem. A*, 2017, **5**, 18326–18378.
21 Kr. Ashurbekova, K. Ashurbekova, I. Saric, E. Modin, M. Petravić, I. Abdulagatov, A. Abdulagatov and M. Knez, *Chem. Commun.*, 2020, **56**, 8778–8781.
22 Kr. Ashurbekova, K. Ashurbekova, I. Saric, M. Gobbi, E. Modin, A. Chuvilin, M. Petravić, I. Abdulagatov and M. Knez, *Chem. Mater.*, 2021, DOI: 10.1021/acs.chemmater.0c04408.
23 Y. Mao and K. K. Gleason, *Langmuir*, 2004, **20**, 2484–2488.
24 M. N. Rocklein and S. M. George, *Anal. Chem.*, 2003, **75**, 4975–4982.
25 D. Seghete, R. A. Hall, B. Yoon and S. M. George, *Langmuir*, 2010, **26**, 19045–19051.
26 D. R. Anderson, in *Analysis of Silicones*, ed. A. L. Smith, Wiley, New York, 1974, p. 247.
27 D. Burkey and K. Gleason, *J. Vac. Sci. Technol., A*, 2004, **22**, 61–70.
28 S. M. Gates, D. A. Neumayer, M. H. Sherwood, A. Grill, X. Wang and M. Sankarapandian, *J. Appl. Phys.*, 2007, **101**, 094103.
29 D. W. Mayo, F. A. Miller and R. W. Hannah, *Course Notes on the Interpretation of Infrared and Raman Spectra*, 2003, pp. 73–84.
30 X. Chen, X. Wang and D. Fang, *Fullerenes, Nanotubes and Carbon Nanostructures*, 2020, vol. 28, pp. 1048–1058.

